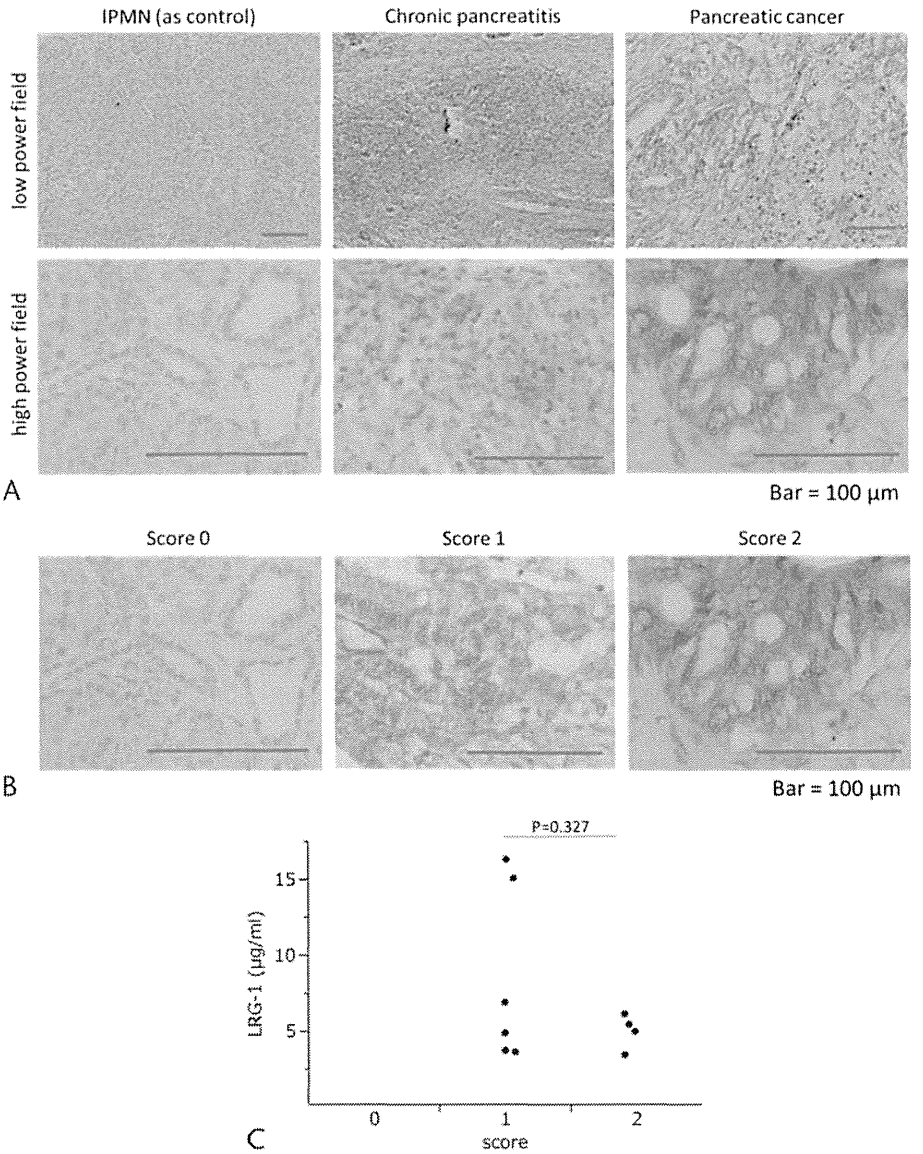

FIGURE 4. Immunohistochemistry of LRG-1 to assess the expression. A, In IPMN cases, the pancreatic duct cells were not stained. In the CP case, the pancreatic duct cells were not stained, but inflammatory cells, such as lymphocytes, stained lightly. In all PDAC cases, the pancreatic cancer cells were stained. Scale bar = 100 μm. B, The intensity of LRG-1 was scored on a scale from 0 to 2 (0, no or faint staining; 1, moderate staining; and 2, strong staining). Scale bar = 100 μm. C, No correlation was found between serum LRG-1 levels and staining intensity ($P = 0.327$).

inhibiting signal transduction through epithelial growth factor receptor and vascular endothelial growth factor have already been developed and are used clinically.[23] More recently, LRG-1 was reported to promote angiogenesis by modulating endothelial TGF-β signaling.[24] These results imply that LRG-1 may be a therapeutic target for controlling pathogenic angiogenesis in cancer.

In conclusion, the present study clearly shows that LRG-1 has promise as a novel tumor biomarker for PDAC.

REFERENCES

1. Jemal A, Siegel R, Xu J, et al. Cancer Statistics, 2010. *CA Cancer J Clin.* 2011;61:133–134.
2. Ministry of Health, Labour and Welfare (2010). The Dynamic Statistics of the Population in 2010. Available at: http://www.mhlw.go.jp/toukei/saikin/hw/jinkou/kakutei11/dl/11_h7.pdf. Accessed December 12, 2012.
3. Wagner M, Redaelli C, Lietz M, et al. Curative resection is the single most important factor determining outcome in patients with pancreatic adenocarcinoma. *Br J Surg.* 2004;91:586–594.
4. Neoptolemos JP, Stocken DD, Bassi C, et al. Adjuvant chemotherapy with fluorouracil plus folinic acid vs gemcitabine following pancreatic cancer resection: a randomized controlled trial. *JAMA.* 2010;304:1073–1081.
5. Jamieson NB, Carter CR, McKay CJ, et al. Tissue biomarkers for prognosis in pancreatic ductal adenocarcinoma: a systematic review and meta-analysis. *Clin Cancer Res.* 2011;17:3316–3331.
6. Humphris JL, Chang DK, Johns AL, et al. The prognostic and predictive value of serum CA19-9 in pancreatic cancer. *Ann Oncol.* 2012;23:1713–1722.
7. Yachida S, Jones S, Bozic I. Distant metastasis occurs late during the genetic evolution of pancreatic cancer. *Nature.* 2010;467:1114–1117.
8. Haupt H, Baudner S. Isolation and characterization of an unknown, leucine-rich 3.1-S-alpha2-glycoprotein from human serum. *Hoppe Seylers Z Physiol Chem.* 1977;358:639–646.
9. Andersen JD, Boylan K, Jemmerson R, et al. Leucine-rich alpha-2-glycoprotein-1 is upregulated in sera and tumors of ovarian cancer patients. *J Ovarian Res.* 2010;3:21.

10. Okano T, Kondo T, Kakisaka T, et al. Plasma proteomics of lung cancer by a linkage of multi-dimensional liquid chromatography and two-dimensional difference gel electrophoresis. *Proteomics*. 2006;6:3938–3948.
11. Sandanayake NS, Sinclair J, Andreola F, et al. A combination of serum leucine-rich α-2-glycoprotein-1, CA19-9 and interleukin-6 differentiate biliary tract cancer from benign biliary strictures. *Br J Cancer*. 2011;105:1370–1378.
12. Sarvari J, Mojtahedi Z, Kuramitsu Y, et al. Differential expression of haptoglobin isoforms in chronic active hepatitis, cirrhosis and HCC related to HBV infection. *Oncol Lett*. 2011;2:871–877.
13. Ladd JJ, Busald T, Johnson MM, et al. Increased plasma levels of the APC-interacting protein MAPRE1, LRG1, and IGFBP2 preceding a diagnosis of colorectal cancer in women. *Cancer Prev Res (Phila)*. 2012;5:655–664.
14. Kakisaka T, Kondo T, Okano T, et al. Plasma proteomics of pancreatic cancer patients by multi-dimensional liquid chromatography and two-dimensional difference gel electrophoresis (2D-DIGE): up-regulation of leucine-rich alpha-2-glycoprotein in pancreatic cancer. *J Chromatogr B Analyt Technol Biomed Life Sci*. 2007;852:257–267.
15. Serada S, Fujimoto M, Terabe F, et al. Serum leucine-rich alpha-2 glycoprotein is a disease activity biomarker in ulcerative colitis. *Inflamm Bowel Dis*. 2012;18:2169–2179.
16. Kharbanda AB, Raj AJ, Cosme Y, et al. Novel serum and urine markers for pediatric appendicitis. *Acad Emerg Med*. 2012;19:56–62.
17. Ai J, Druhan LJ, Hunter MG, et al. LRG-accelerated differentiation defines unique G-CSFR signaling pathways downstream of PU.1 and C/EBPepsilon that modulate neutrophil activation. *J Leukoc Biol*. 2008;83:1277–1285.
18. Kentsis A, Ahmad S, Kurek K, et al. Detection and diagnostic value of urine leucine-rich α-2-glycoprotein in children with suspected acute appendicitis. *Ann Emerg Med*. 2012;60:78–83.
19. Kawakami T, Hoshida Y, Kanai F, et al. Proteomic analysis of sera from hepatocellular carcinoma patients after radiofrequency ablation treatment. *Proteomics*. 2005;5:4287–4295.
20. Takahashi N, Takahashi Y, Putnam FW. Periodicity of leucine and tandem repetition of a 24-amino acid segment in the primary structure of leucine-rich alpha 2-glycoprotein of human serum. *Proc Natl Acad Sci*. 1985;82:1906–1910.
21. Shirai R, Gotou R, Hirano F, et al. Autologous extracellular cytochrome c is an endogenous ligand for leucine-rich α2-glycoprotein and β-type phospholipase A2 inhibitor. *J Biol Chem*. 2010;285:21607–21614.
22. Codina R, Vanasse A, Kelekar A, et al. Cytochrome c-induced lymphocyte death from the outside in: inhibition by serum leucine-rich alpha-2-glycoprotein-1. *Apoptosis*. 2010;15:139–152.
23. Kim ST, Park KH, Shin SW, et al. Dose KRAS mutation status affect on the effect of VEGF therapy in metastatic colon cancer patients? *Cancer Res Treat*. 2014;46:48–54.
24. Wang X, Abraham S, McKenzie JA, et al. LRG1 promotes angiogenesis by modulating endothelial TGF-b signaling. *Nature*. 2013;499:306–311.

Rheumatology Advance Access published August 28, 2014
RHEUMATOLOGY 262
Original article doi:10.1093/rheumatology/keu325

Proteomic identification of heterogeneous nuclear ribonucleoprotein K as a novel cold-associated autoantigen in patients with secondary Raynaud's phenomenon

Lingli Yang[1,2], Minoru Fujimoto[2], Hiroyuki Murota[1], Satoshi Serada[2], Manabu Fujimoto[3], Hiromi Honda[2], Kohji Yamada[2,4], Katsuya Suzuki[5], Ayumi Nishikawa[5], Yuji Hosono[6], Yoshihiro Yoneda[7], Kazuhiko Takehara[3], Yoshitaka Imura[6], Tsuneyo Mimori[6], Tsutomu Takeuchi[5], Ichiro Katayama[1] and Tetsuji Naka[2]

Abstract

Objective. The aim of this study was to identify cold-associated autoantibodies in patients with RP secondary to CTDs.

Methods. Indirect immunofluorescence staining was performed on non-permeabilized cold-stimulated normal human dermal microvascular endothelial cells (dHMVECs), using patients' sera. Cold-induced alterations in cell surface proteomes were analysed by isobaric tag for relative and absolute quantitation (iTRAQ) analysis. Serological proteome analysis (SERPA) was applied to screen cold-associated autoantigens. The prevalence of the candidate autoantibody was determined by ELISA in 290 patients with RP secondary to CTDs (SSc, SLE or MCTD), 10 patients with primary RP and 27 healthy controls.

Results. Enhanced cell surface immunoreactivity was detected in cold-stimulated dHMVECs when incubated with sera from patients with secondary RP. By iTRAQ analysis, many proteins, including heterogeneous nuclear ribonucleoprotein K (hnRNP-K), were found to be increased on the cell surface of dHMVECs after cold stimulation. By the SERPA approach, hnRNP-K was identified as a candidate autoantigen in patients with secondary RP. Cold-induced translocation of hnRNP-K to the cell surface was confirmed by immunoblotting and flow cytometry. By ELISA analysis, patients with secondary RP show a significantly higher prevalence of anti-hnRNP-K autoantibody (30.0%, 61/203) than patients without RP (9.2%, 8/87, $P = 0.0001$), patients with primary RP (0%, 0/10, $P = 0.0314$) or healthy controls (0%, 0/27, $P = 0.0001$).

Conclusion. By comprehensive proteomics, we identified hnRNP-K as a novel cold-associated autoantigen in patients with secondary RP. Anti-hnRNP-K autoantibody may potentially serve as a biomarker for RP secondary to various CTDs.

Key words: proteomics, Raynaud's phenomenon, autoantibody, heterogeneous nuclear RNP-K.

[1]Department of Dermatology, Osaka University Graduate School of Medicine, [2]Laboratory of Immune Signal, National Institute of Biomedical Innovation, [3]Department of Dermatology, Kanazawa University, Kanazawa, [4]Biomolecular Dynamics Group, Graduate School of Frontier Biosciences, Osaka University, Osaka, [5]Division of Rheumatology, Department of Internal Medicine, Keio University School of Medicine, Tokyo, [6]Department of Rheumatology and Clinical Immunology, Graduate School of Medicine, Kyoto University, Kyoto and [7]National Institute of Biomedical Innovation, Osaka, Japan.

Submitted 4 November 2013; revised version accepted 23 June 2014.

Correspondence to: Tetsuji Naka, Laboratory of Immune Signal, National Institute of Biomedical Innovation, 7-6-8, Saito-asagi, Ibaraki, Osaka 567-0085, Japan. E-mail: tnaka@nibio.go.jp

Lingli Yang, Minoru Fujimoto, Hiroyuki Murota and Satoshi Serada contributed equally to this study.

Introduction

Advances in proteomics technologies have enabled us to identify proteins extracted from various clinical samples. Recently an innovative multiplexed quantitative proteomic technology called isobaric tag for relative and absolute quantification (iTRAQ) has been successfully used to detect disease-related proteins from cultured cells and clinical samples [1]. This novel technology can not only identify proteins in samples, but also compare relative expression levels of detected proteins from between four to eight different samples [2]. In addition, when samples enriched with cell surface proteins are analysed, iTRAQ technology can characterize differences in cell surface proteomes between samples [3].

RP is an exaggerated vasoconstrictive response of the fingers and toes to external stress such as cold temperatures [4]. RP is characterized classically as the episodic colour change of blanching, cyanosis and rubor in response to external stress [5]. In most patients, this colour change is a benign, reversible condition and no underlying disease is detectable (i.e. primary RP) [4]. However, in some patients RP is the early manifestation of underlying disease (i.e. secondary RP), most frequently of CTDs, including SSc [4], SLE [6] and MCTD [7]. RP in CTD patients is more severe than primary RP and causes tissue damage, including digital ulcers and gangrene, presumably due to endothelial abnormalities [8]. Moreover, given the substantial morbidity in patients with CTDs, RP patients developing CTDs should be promptly identified and managed. Thus it is important to distinguish between primary and secondary RP, but the diagnostic methods have not been established.

Because autoantibody production is a common hallmark of CTDs, RP secondary to CTDs might have a similar autoimmune pathogenesis. We therefore hypothesized that cold stimulation, as an environmental cue, may contribute to the triggering of local autoimmune reactions in patients with CTD-related secondary RP. In this study, taking advantage of iTRAQ technology, we detected cold-induced alteration in cell surface proteomes of endothelial cells. We then obtained candidate autoantigens in RP by serological proteome analysis (SERPA) [9–11] combining two-dimensional electrophoresis and western blotting using patients' sera. Our analyses collectively suggest that in patients with secondary RP, heterogeneous nuclear ribonucleoprotein K (hnRNP-K) is a cold-associated autoantigen that translocates onto the cell surface by cold stimulation.

Materials and methods

Human serum samples

Between March 2003 and January 2012, Japanese patients referred to hospitals of Osaka University (Osaka, Japan), Kyoto University (Kyoto, Japan), Kanazawa University (Kanazawa, Japan) and Keio University (Tokyo, Japan) were newly evaluated for RP as well as for SSc according to ACR criteria [12], SLE according to ACR criteria [13, 14] or MCTD according to the criteria proposed by the Ministry of Health and Welfare in Japan [15]. RP was defined by repeated episodes of biphasic or triphasic colour change on cold exposure and non-RP was defined by no colour changes on cold exposure, as described previously [16]. The possible RP of unilateral or uniphasic colour change was not included in this study. After these exclusions, randomly selected patients, including 155 well-defined SSc with RP [SSc-RP(+)] patients, 54 SLE without RP [SLE-RP(−)] patients, 1 MCTD without RP [MCTD-RP(−)] patient and 10 MCTD with RP [MCTD-RP(+)] patients, were included in this study. SSc without RP [SSc-RP(−)] patients ($n = 32$) and SLE with well-defined RP [SLE-RP(+)] ($n = 38$) patients, the frequencies of which are substantially low, were intentionally recruited and included in the study. Sera and characteristics (demographic characteristics, autoantibody profile) of CTD patients were collected at the time of diagnosis. Ten patients with primary RP who had well-defined RP for >2 years and had normal findings on laboratory tests, negative findings on autoantibody assays and no objective clinical signs of CTD or other diseases were also included. These patient characteristics are summarized in Table 1. As controls, healthy individuals with no evidence of any physical disorder were included [$n = 27$; male:female ratio 3:24, average age 51.0 years (S.D. 13.2)]. All patients gave written informed consent prior to inclusion and this study was approved by the Medical Ethics Committees of the National Institute of Biomedical Innovation (Osaka, Japan), Osaka University Hospital, Kyoto University Hospital, Kanazawa University Hospital and Keio University Hospital.

Cell culture and cold stimulation

Normal human dermal microvascular (MV) endothelial cells (dHMVECs, passages 4–6) were purchased from Takara Bio (Otsu, Japan). dHMVECs were cultured on type 1 collagen-coated plates (Iwaki Glass, Tokyo, Japan) in endothelial basal medium 2 supplemented with endothelial cell growth medium 2 MV SingleQuots (Clonetics, San Diego, CA, USA). Confluent dHMVECs cells were incubated in serum-containing medium at 10°C (cold stress) or 37°C (control) in a 5% CO_2 humidified incubator for the periods indicated. Cells were maintained at 10°C or 37°C during the washing/detachment procedure. Suspended cells were then harvested by centrifugation at room temperature. Before and after cold stimulation, cell viability was verified by trypan blue exclusion assay. In some experiments, cells were further fixed with 4% paraformaldehyde at room temperature.

Indirect immunofluorescence staining

dHMVECs were seeded on six-well plates precoated with type 1 collagen (5×10^4 cells/well) and grown to confluence. Cells were fixed with 4% paraformaldehyde. Non-permeabilized cells were then incubated with sera from patients and healthy controls (HCs; 1:500 dilution) for 1 h at room temperature, followed by incubation with FITC-conjugated rabbit anti-human IgG (1:1000 dilution;

TABLE 1 Patient characteristics ($n = 300$ with CTDs or primary RP)

Variable	SSc ($n = 187$)	SLE ($n = 92$)	MCTD ($n = 11$)	Primary RP ($n = 10$)
Age, mean (S.D.), years	55.3 (13.8)	40.3 (14.9)	59.5 (16.3)	25.4 (3.1)
Gender (F:M), *n:n*	156:31	86:6	11:0	9:1
Smoking, % (*n/N*)	44.2 (50/163)	25.8 (16/46)	0 (0/11)	0 (0/10)
ANA positivity, % (n/N)	91.4 (167/183)	96.7 (89/92)	100 (10/10)	0 (0)
Anti-Scl-70, % (*n/N*)	31.0 (58/187)	NA	NA	0 (0/10)
Anti-centromere, % (*n/N*)	33.7 (63/187)	NA	9.1 (1/11)	0 (0/10)
Anti-Sm, % (*n/N*)	NA	34.5 (30/87)	9.1 (1/11)	NA
Anti-dsDNA, % (*n/N*)	NA	65.1 (54/83)	0 (0/3)	NA
Anti-U1-RNP, % (*n/N*)	7.5 (14/187)	50.0 (43/86)	100.0 (11/11)	0 (0/10)
Anti-SSA/Ro, % (*n/N*)	7.5 (14/187)	57.8 (52/87)	45.5 (5/11)	NA

Scl-70: topoisomerase I; Sm: Smith; U1-RNP: U1 ribonucleoprotein; *N*: the number of available patients (varies according to the number of available observations); NA: not available.

Dako Immunoglobulins, Copenhagen, Denmark). Cells counterstained with Hoechst 33342 (Invitrogen, Carlsbad, CA, USA) were visualized using a Biozero microscope (Keyence, Itasca, IL, USA).

Capture of cell surface proteins

After cold stimulation (10°C) for the indicated periods (0 min, 30 min, 1 h, 3 h), dHMVECs were washed with pre-warmed (37°C) or precooled (10°C) PBS three times and cell surface proteins were then labelled by biotinylation and pulled down by avidin–agarose resin as described previously [3]. The isolated cell surface proteins were kept at −20°C until use.

iTRAQ analysis

Cell surface proteins described above were digested by trypsin and separately labelled with the iTRAQ reagent (Applied Biosystems, Foster City, CA, USA) as described previously [3]. Briefly, iTRAQ reagents 114–117 were used to label cells without cold stimulation (baseline), cells with cold stimulation at 10°C for 30 min, cells with cold stimulation at 10°C for 1 h and cells with cold stimulation at 10°C for 3 h, respectively. Samples were then pooled and fractionated by strong cation exchange chromatography [3]. Nano liquid chromatography–tandem mass spectrometry (LC-MS/MS) analyses were performed on an LTQ-Orbitrap XL (Thermo Fisher Scientific, Waltham, MA, USA) as described previously [3]. Protein identification and quantification for iTRAQ analysis were carried out using Proteome Discoverer software (version 1.1; Thermo Fisher Scientific) against the Swiss Prot protein database [SwissProt 2010_10 (521 016 sequences)] as described previously [3] with modifications as follows: carbamidomethylation and iTRAQ4plex (Lys, N-terminal) were specified as static modifications, whereas CAMthiopropanoyl (Lys, N-terminal), iTRAQ4plex (Tyr) and oxidation (Met) were specified as variable modifications in the database search. The mass spectrometry raw data and the data of peptide identifications were uploaded to PeptideAtlas (http://www.peptideatlas.org/PASS/PASS00387). Information about the subcellular localization of detected proteins was obtained by using UniprotKB (http://www.uniprot.org/).

Serological proteome analysis

Proteins were extracted from cultured dHMVECs using the Complete Mammalian Proteome Extraction Kit (Calbiochem, La Jolla, CA, USA) and stored at −80°C until use. Two-dimensional electrophoresis and immune blotting analysis using patient or HC sera were performed as previously described [10, 11]. Protein spots in a silver-stained gel, corresponding to positive spots on western blot membranes, were excised from the gel and digested in gel as described previously [17].

Preparation of recombinant human hnRNP-K

Full-length hnRNP-K cDNA was amplified from total cDNA of dHMVEC using KOD-plus (Toyobo, Osaka, Japan) with the following primers: 5′-TGGAAACTGAACAGCCAGAAG AA-3′ (forward) and 5′-GCATTAGAATCCTTCAACATCTG C-3′ (reverse). Full-length hnRNP-K cDNA was subcloned into a pET28 vector (Novagen, Madison, WI, USA), resulting in expression of hnRNP-K with a 6 × His tag. The DNA sequence was confirmed using the ABI Prism 3130XL Genetic Analyzer (Applied Biosystems). Recombinant protein was produced in *Escherichia coli* as described previously [10, 11].

ELISA

The ELISA assay was performed using MaxiSorp plates (Nunc A/S, Roskilde, Denmark) coated with 1 μg/well of recombinant human full-length hnRNP-K protein. After dilution (1:500) with *E. coli* cell lysates to block the non-specific reactivity of sera with bacterial proteins, sera were incubated with plate-bound hnRNP-K for 1 h, followed by detection of antigen–antibody complexes by horseradish peroxidase (HRP)-conjugated rabbit anti-human IgG (Dako, Carpinteria, CA, USA) as described previously [10, 11]. Optical density (OD) was read at 450 nm on a Model 680 Microplate Reader (Bio-Rad Laboratories, Hercules, CA, USA). The antibody titre was expressed using arbitrary binding units calculated

according to the following formula: binding units of sample = [OD_{sample}/(mean $OD_{HC\ sera}$ + 3 S.D.$_{HC\ sera}$)] × 100. Based on this formula, 100 binding units was used as the cut-off point.

Western blot analysis

Extracted proteins were subjected to western blot analysis as previously described [18] with the following antibodies: serum at 1:200 dilution; anti-hnRNP-K (1:500 dilution; Cell Signaling Technology, Danvers, MA, USA); anti-VE-cadherin (1:500 dilution; BD Transduction Laboratories, San Jose, CA, USA); anti-glyceraldehyde-3-phosphate dehydrogenase (GAPDH; 1:1000 dilution; Santa Cruz Biotechnology, Dallas, TX, USA), followed by rabbit anti-human IgG, donkey anti-rabbit or sheep anti-mouse HRP-conjugated secondary antibodies (1:5000 dilution; GE Healthcare, Piscataway, NJ, USA) and visualized with Western Lightning Plus ECL reagent (Perkin-Elmer, Boston, MA, USA).

Fluorescence-activated cell sorting

After stimulation, cells fixed with 4% paraformaldehyde were incubated with rabbit anti-human hnRNP-K antibody at 1:100 dilution and labelled with FITC-conjugated goat anti-rabbit immunoglobulin (BD Biosciences, San Jose, CA, USA). Normal rabbit IgG was used as a control. Stained cells were analysed using a FACS Canto II cytometer (Becton-Dickinson, Mountain View, CA, USA) and the results were analysed using FlowJo software (TreeStar, Ashland, OR, USA).

Statistical analysis

Continuous variables are expressed as mean (S.D.) and proportions were used for categorical variables. Means were compared with Student's *t*-test, highly skewed distributions were compared using the Mann–Whitney *U* test and proportions were compared using Fisher's exact test. Differences between groups were compared using the Kruskall–Wallis test followed by Steel's test. The data were entered and analysed using Excel statistical software (Microsoft, Redmond, WA, USA). Significance was defined as $P < 0.05$.

Results

Cold-induced autoimmune reactions on the cell surface

To determine whether cold can affect autoimmune reactions on the surface of vascular endothelial cells, non-permeabilized dHMVECs pretreated with or without cold stimulation were incubated with sera from patients with RP secondary to SSc or HCs. By indirect immunofluorescence staining using sera from patients, cell surface immunoreactivity was strongly induced in cold-stimulated dHMVECs (eight of nine patients with SSC-related RP; Fig. 1), but not in unstimulated cells. In contrast, no distinct immunostaining was observed in cold-stimulated or unstimulated cells when incubated with sera from HCs ($n = 3$; Fig. 1). These results indicate that pretreatment of dHMVECs with cold is critical in inducing the interaction between cell surface autoantigens and sera from patients.

Fig. 1 Indirect immunofluorescence staining

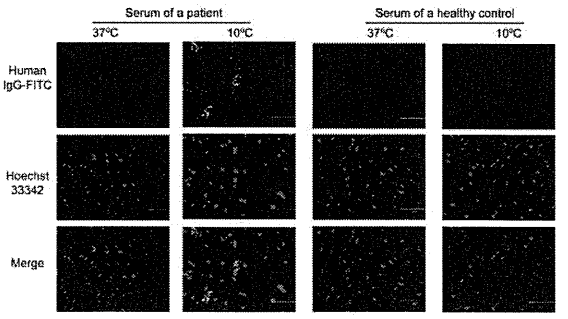

Non-permeabilized cultured dHMVECs with or without cold stimulation were incubated with sera (1:500 dilution) from patients with SSc-related secondary RP ($n = 9$) or healthy controls ($n = 3$) (×100 magnification). Representative images are shown here. FITC-conjugated rabbit anti-human IgG (green); Hoechst 33342 (blue); bar: 100 μm. dHMVECs: dermal human microvascular endothelial cells.

Identification of cold-induced surface proteome alterations in dHMVECs by iTRAQ analysis

The results above suggest that proteins including autoantigens in dHMVECs might be exposed to the cell surface in response to cold stimulation. Therefore we next investigated cold-induced cell surface proteome alterations in dHMVECs. Cells were stimulated with cold (10°C for 0 min, 30 min, 1 h and 3 h) and cell surface proteins enriched by a biotinylation-based approach were quantitatively analysed by iTRAQ technology using nano LC-MS/MS analysis. As listed in supplementary Table S1, available at *Rheumatology* Online, 1581 proteins were identified. According to the annotation from UniprotKB, 451 proteins (28.5%) are located mainly in the plasma membrane, 503 proteins (31.8%) in the cytoplasm, 238 proteins (15.1%) in the nucleus and the remaining proteins (24.6%) in other subfractions such as the mitochondrion and the endoplasmic reticulum. The expression of ~50% of the proteins increased >2-fold after cold stimulation at 10°C for 3 h (see supplementary Table S1, available at *Rheumatology* Online). The top 30 highly increased proteins are listed in Table 2.

Identification of autoantigens by SERPA in patients with secondary RP

We then used a SERPA approach to screen autoantigens associated with secondary RP. At first, proteins from dHMVEC lysates were separated on two-dimensional gels and were visualized by silver staining (Fig. 2A) or were transferred to membranes for immunoblotting. These membranes were incubated with sera from nine

TABLE 2 List of differentially expressed proteins on the cell surface of dHMVECs after cold stimulation

Accession	Protein name	0.5 h	1 h	3 h
Q96RS6	NudC domain-containing protein 1	3.25	4.24	6.18
P10301	Ras-related protein R-Ras	1.35	3.90	5.95
Q92797	Symplekin	2.94	3.81	5.54
Q643R3	Lysophospholipid acyltranferase LPCAT4	3.06	3.00	5.45
Q99808	Equilibrative nucleoside transporter 1	2.62	3.69	5.21
Q9Y6I9	Testis-expressed sequence 264 protein	2.66	4.11	5.12
Q8TEQ6	Gem-associated protein 5	4.71	6.03	5.08
Q2TAL8	Glutamine-rich protein 1	3.03	4.56	4.99
Q08379	Golgin subfamily A member 2	2.41	4.10	4.74
P49916	DNA ligase 3	2.52	2.94	4.74
P35659	Protein DEK	2.04	3.65	4.67
O60264	SWI/SNF-related matrix-associated actin-dependent regulator of chromatin subfamily A member 5	1.87	4.38	4.52
P60709	Actin, cytoplasmic 1	3.03	3.67	4.28
P55265	Double-stranded RNA-specific adenosine deaminase	2.22	3.86	4.27
Q16643	Drebrin	2.60	3.75	4.24
Q6DD88	Atlastin-3	2.09	3.83	4.14
P29966	Myristoylated alanine-rich C-kinase substrate	1.89	3.61	4.10
Q9ULT8	E3 ubiquitin-protein ligase HECTD1	1.74	3.63	4.08
P61019	Ras-related protein Rab-2A	2.04	3.63	4.03
P61978	hnRNP-K	2.12	3.75	4.03
P01112	GTPase HRas	1.68	2.01	3.95
Q07666	KH domain-containing, RNA-binding, signal transduction-associated protein 1	1.74	3.54	3.92
Q9NZ01	Trans-2,3-enoyl-CoA reductase	1.77	2.08	3.89
Q9NQW6	Actin-binding protein anillin	3.78	5.01	3.86
O00483	NADH dehydrogenase [ubiquinone] 1 alpha subcomplex subunit 4	2.12	2.94	3.86
Q9NP72	Ras-related protein Rab-18	1.96	3.20	3.83
O94901	Protein unc-84 homolog A	2.04	2.77	3.79
P38646	Stress-70 protein, mitochondrial	1.83	3.39	3.76
Q96S97	Myeloid-associated differentiation marker	2.49	3.10	3.75
P49585	Choline-phosphate cytidylyltransferase A	2.68	3.62	3.74

Values are shown as relative expression levels (at 10°C for 0.5, 1 and 3 h) compared with baseline (at 37°C). dHMVECs: dermal human microvascular endothelial cells; hnRNP-K: heterogeneous nuclear ribonucleoprotein K.

patients with RP secondary to SSc (Fig. 2B) or three HCs (Fig. 2C). Six specific spots, which were recognized by sera from >75% of patients, but not by those from HCs, were selected (Fig. 2B). Proteins extracted from the corresponding spots on the silver-stained gel (Fig. 2A) were then subjected to LC-MS/MS analysis and candidate autoantigens were identified by a database search as detailed in Fig. 2D. Among identified candidates, hnRNP-K, a member of the nuclear proteins involved in nucleic acid metabolism [19], was also found in the list of increased proteins on the cell surface under cold stimulation (Table 2), suggesting that hnRNP-K might be a cold-related autoantigen in patients with secondary RP.

Cell surface expression of hnRNP-K under cold stimulation was confirmed by western blot and FACS analysis

The hnRNP proteins are among the most abundant proteins in the nucleus [20]. Indeed, hnRNP-K in dHMVECs under physiological culture conditions was stained intensely in the nucleus by immunofluorescence analysis (see supplementary Fig. S1A and B, available at *Rheumatology* Online). Cold stimulation (10°C for 3 h) induced extranuclear localization of hnRNP-K (see supplementary Fig. S1C and D, available at *Rheumatology* Online), which was nonetheless overwhelmed by intensive staining of nuclear hnRNP-K. To investigate further the appearance of hnRNP-K on the cell surface after cold stimulation, we next performed western blot and FACS analysis. By western blot analysis using concentrated cell surface proteins, hnRNP-K clearly increased in dHMVECs after cold stimulation, but VE-cadherin did not (Fig. 3A). In contrast, the expression level of total hnRNP-K was found to be unchanged during cold stimulation, suggesting that hnRNP-K was not newly synthesized after cold stimulation (Fig. 3A). By FACS analysis, cold-induced expression of hnRNP-K on the cell surface was further confirmed (Fig. 3B). These results collectively suggest that hnRNP-K is a protein that translocates to the cell surface on cold stimulation.

FIG. 2 Identification of autoantigens by SERPA

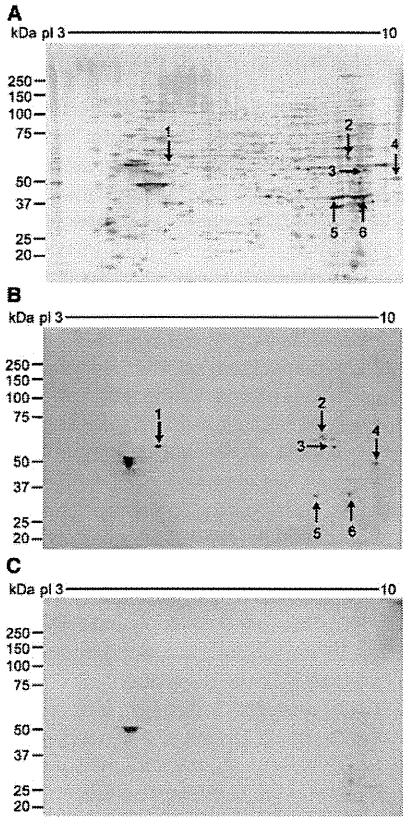

D

no.	Access	Identified protein	Mw(kDa)	PI	Coverage(%)
1	P48643	T-complex protein 1 subunit epsilon	59.63	5.66	30.13
	P61978	Heterogeneous nuclear ribonucleoprotein K	50.94	5.54	19.44
	P10809	60 kDa heat shock protein, mitochondrial	61.92	5.87	16.40
	Q13283	Ras GTPase-activating protein-binding protein 1	52.13	5.52	18.03
	Q92769	Histone deacetylase 2	55.33	5.91	13.11
	Q9H0R6	Glutamyl-tRNA(Gln) amidotransferase subunit A homolog	57.42	5.68	11.55
	Q05682	Caldesmon	93.19	5.67	3.15
	O15460	Prolyl 4-hydroxylase subunit alpha-2	60.86	5.71	4.11
	Q9UN86	Ras GTPase-activating protein-binding protein 2	54.09	5.55	5.19
2	P29401	Transketolase	67.83	7.66	8.19
	P49748	Very long-chain specific acyl-CoA dehydrogenase, mitochondrial	70.35	8.75	4.27
	Q92804	TATA-binding protein-associated factor 2N	61.79	8.02	7.77
3	P14618	Pyruvate kinase isozymes M1/M2	57.90	7.84	25.05
	P50991	T-complex protein 1 subunit delta	57.89	7.83	11.13
	Q14554	Protein disulfide-isomerase A5	59.56	7.91	11.75
	Q99832	T-complex protein 1 subunit eta	59.33	7.65	11.60
	Q9H078	Caseinolytic peptidase B protein homolog	78.68	9.01	7.64
	P06744	Glucose-6-phosphate isomerase	63.11	8.32	4.30
4	P68104	Elongation factor 1-alpha 1	50.11	9.01	16.45
	P06733	Alpha-enolase	47.14	7.39	9.45
	P55084	Trifunctional enzyme subunit beta, mitochondrial	51.26	9.41	6.12
5	P00338	L-lactate dehydrogenase A chain	36.67	8.27	33.13
	Q14192	Four and a half LIM domains protein 2	32.17	7.55	34.41
	P07355	Annexin A2	38.58	7.75	20.06
	P40926	Malate dehydrogenase, mitochondrial	35.48	8.68	18.05
	P22626	Heterogeneous nuclear ribonucleoproteins A2/B1	37.41	8.95	10.20
	P53597	Succinyl-CoA ligase [GDP-forming] subunit alpha, mitochondrial	36.23	8.79	8.67
	Q16270	Insulin-like growth factor-binding protein 7	29.11	7.90	11.70
6	P04406	Glyceraldehyde-3-phosphate dehydrogenase	36.03	8.46	11.94
	P22626	Heterogeneous nuclear ribonucleoproteins A2/B1	37.41	8.95	10.76
	Q9UKM9	RNA-binding protein Raly	32.44	9.17	8.82
	P23193	Transcription elongation factor A protein 1	33.95	8.38	10.30
	P07355	Annexin A2	38.58	7.75	6.19

(**A**–**C**) Total protein extracts of dHMVECs were separated by two-dimensional PAGE followed by silver staining analysis (**A**) or by western blot analysis with diluted sera from SSc patients with RP (**B**) or from healthy controls (**C**). Arrows and numbers indicate protein spots that were recognized only by the patients' sera. Representative images are shown here. (**D**) List of proteins identified by LC-MS/MS analysis (Mw: molecular weight; pI: isoelectric point). dHMVECs: dermal human microvascular endothelial cells; LC-MS/MS: liquid chromatography–tandem mass spectrometry.

Detection of anti-hnRNP-K antibody in sera from patients with secondary RP by western blot and ELISA analysis

To confirm that hnRNP-K is the autoantigen recognized by sera from patients with secondary RP, full-length recombinant human hnRNP-K protein was prepared and subjected to western blot analysis. As disease controls, SSc patients without RP were intentionally recruited to the study and their sera were investigated. Notably, intense reactivity against recombinant hnRNP-K protein was visualized in sera from SSc patients with RP, but not sera from SSc patients without RP or from HCs (Fig. 3C). This result implies that anti-hnRNP-K antibody is relevant to RP rather than to SSc itself.

We then developed an ELISA system using recombinant hnRNP-K protein to screen anti-hnRNP-K antibody in various CTD patients (SSc, SLE and MCTD) with or without RP and in patients with primary RP (Table 1). As shown in Fig. 3D (top), ELISA analysis revealed that significant elevations of anti-hnRNP-K antibody levels were observed in patients with SSc-, SLE- and MCTD-related RP, but not in patients without RP or those with primary RP compared with HCs (Fig. 3D, top). The prevalence of autoantibodies against hnRNP-K was 26.5% in SSc patients with RP, 42.1% in SLE patients with RP and 40.0% in MCTD patients with RP. In contrast, anti-hnRNP-K positivity was markedly low in CTD patients without RP and was 0% in primary RP patients and HCs (Fig. 3D, top). These results suggest that anti-hnRNP-K antibody is relevant to CTD-related secondary RP rather than to a single CTD.

Of all the CTDs (SSc, SLE and MCTD) in this study, a 30.0% prevalence of anti-hnRNP-K antibody was observed in patients with RP, much higher than that in patients without RP (9.20%, $P = 0.0001$), in patients with primary RP (0%, $P = 0.0314$) or in HCs (0%, $P = 0.0003$) (Fig. 3D, bottom). Anti-hnRNP-K-positive CTD patients had a significantly higher prevalence of RP (88.4%) than

FIG. 3 Cell surface expression of hnRNP-K after cold stimulation and the presence of anti-hnRNP-K autoantibody in sera from patients with secondary RP

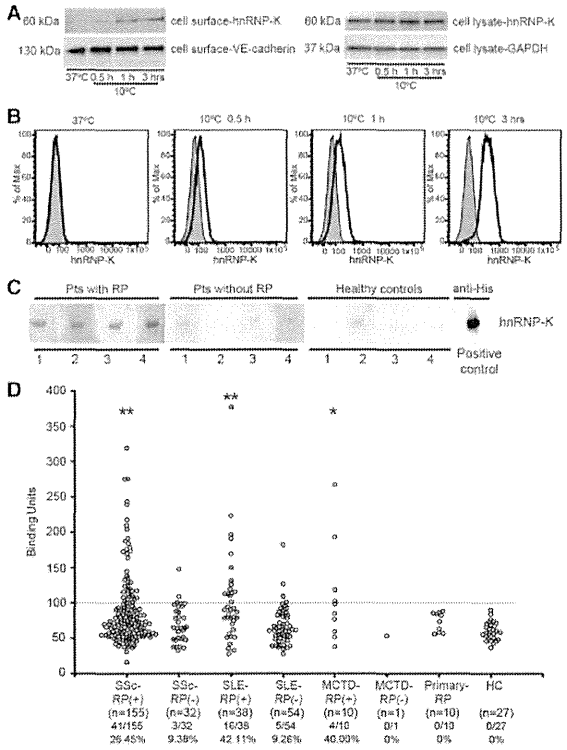

		anti-hnRNP-K	
		Positive	Negative
CTD-RP(+)	n=203	61 (30.0%) †	142 (70.0%)
CTD-RP(-)	n=87	8 (9.20%)	79 (90.8%)
Primary RP	n=10	0 (0%)	10 (100%)
HC	n=27	0 (0%)	27 (100%)

(**A**) Biotinylated surface proteins from dHMVECs incubated at 37°C or 10°C (indicated periods) were precipitated with streptavidin-conjugated agarose beads and analysed by western blot analysis using anti-hnRNP-K. Levels of VE-cadherin surface protein (left panel) and GAPDH expression in total cell lysates (right panel) are shown as controls. (**B**) Cell surface hnRNP-K expression in dHMVECs was analysed by flow cytometry. Shaded histogram indicates staining with control IgG. (**C**) His-tagged recombinant hnRNP-K protein was subjected to western blot analysis using diluted sera from SSc patients with RP, without RP and healthy controls or with anti-6 × His antibody. (**D**) (Top) Serum anti-hnRNP-K antibody levels in indicated CTD patients (with or without RP), primary RP patients and healthy controls were determined by ELISA using recombinant human hnRNP-K. The *y*-axis denotes binding units. The solid horizontal line indicates the positive cut-off limit as described in Materials and methods. Note that this cohort contains a relatively high number of SSc without RP patients and SLE with RP patients, because those patients were intentionally recruited to this study. $^{*}P < 0.05$, $^{**}P < 0.01$ *vs* HCs. (Bottom) Anti-hnRNP-K positivity in patients is summarized. CTD patients are combined here. Values are the number (%) of patients. †$P = 0.00001$ *vs* CTD-RP(−), $P = 0.0314$ *vs* primary RP, $P = 0.0001$ *vs* HCs by Fisher's exact test.

dHMVECs: dermal human microvascular endothelial cells; hnRNP-K: heterogeneous nuclear ribonucleoprotein K; GAPDH: glyceraldehyde-3-phosphate dehydrogenase.

anti-hnRNP-K-negative patients (64.3%, $P = 0.0001$; Table 3). Anti-hnRNP-K antibody showed no correlation with age, gender, smoking or antibodies to U1 ribonucleoprotein (U1-RNP), centromere or SSA/Ro in CTD patients (Table 3). In addition, anti-hnRNP-K showed no correlation with autoantibodies against topoisomerase I (Scl-70) in SSc patients or those against dsDNA or Sm in SLE patients (data not shown). Thus anti-hnRNP-K antibody might be a novel class of biomarker for a subgroup of patients with CTD-related secondary RP.

Discussion

Environmental factors are implicated in the pathogenesis of autoimmune diseases. Previously translocation of intracellular autoantigens to the cell surface was described in ultraviolet radiation-stimulated keratinocytes [21–23]. In the present study, using comprehensive proteomics approaches, we identified hnRNP-K as a novel autoantigen that translocates to the cell surface of dHMVECs after cold stimulation. ELISA analysis revealed that anti-hnRNP-K antibody was significantly elevated in patients with RP secondary to CTDs, but not in patients with primary RP. Thus our data imply hnRNP-K is a putative secondary RP-associated autoantigen that is exposed on the cell surface by cold stimulation.

iTRAQ analysis indicated that cold stimulation in dHMVECs could induce cell surface expression of a variety of proteins, including intracellular proteins, without an overt effect on cell viability, as seen by trypan blue exclusion assay (data not shown). Previous lines of evidence indicate that cytoplasmic and nuclear proteins can reach the cell surface by Golgi-independent non-conventional transport pathways [24–26]. However, it is unknown how cold stimulation induces the translocation of hnRNP-K and other intracellular proteins. Further study is currently under way in our laboratory.

Among many up-regulated proteins identified by iTRAQ analysis, hnRNP-K was the only protein simultaneously identified by SERPA screening. However, our study does not exclude the possibility that there remain other cold-associated autoantigens among these proteins. In particular, since the SERPA approach has limitations in detecting native antigens, antibodies that recognize only native-form autoantigens might have been missed in our study. A screening strategy other than SERPA is necessary to clarify this issue.

hnRNP-K is a 464 amino acid nuclear protein with three K homology domains that mediate DNA and RNA binding [27]. Autoantibodies to hnRNP-K have previously been detected in sera from patients with aplastic anaemia and

TABLE 3 Basic information of 290 patients with CTDs according to the presence of anti-hnRNP-K antibodies

Variable	Positive ($n = 69$)	Negative ($n = 221$)	P value*
Age, mean (S.D.), years	52.4 (15.6)	53.3 (15.4)	0.3613
Gender (F:M), *n:n*	61:8	192:29	0.8383
Smoking, % (*n/N*)	18.9 (10/53)	31.6 (56/177)	0.0841
RP, % (*n*)	88.4 (61)	64.3 (142)	0.0001
ANA positivity, % (*n/N*)	94.0 (63/67)	93.1 (203/218)	1.0000
Anti-U1-RNP, % (*n/N*)	26.5 (18/68)	23.1 (50/166)	0.6255
Anti-SSA/Ro positivity, % (*n/N*)	27.9 (19/68)	23.6 (52/220)	0.5202

*Univariate analysis using the Mann–Whitney U test or Fisher's exact test. *N*: the number of available patients (varies according to the number of available observations). hnRNP-K: heterogeneous nuclear ribonucleoprotein K.

RA (31% and 24%, respectively), although the co-morbidity of RP in these patients was not described in this report [28]. Autoantibodies to other hnRNPs such as hnRNP-H1 [29], -B1 and -F [30] have also been reported as possible diagnostic markers of CTDs, but their relevance to RP has not been examined.

Although anti-hnRNP-K antibody was identified initially using sera from patients with SSc-related RP, this autoantibody was also detected in sera from RP patients with other CTDs. Notably, anti-hnRNP-K antibody levels in RP patients secondary to SSc, SLE and MCTD were significantly higher than in HCs. In addition, the prevalence of anti-hnRNP-K antibody in SSc patients with RP (26.5%), SLE patients with RP (42.1%) and MCTD patients with RP (40.0%) was markedly higher than in their RP-negative counterparts (9.4%, 9.3% and 0%, respectively) and in primary RP patients (0%). Moreover, anti-hnRNP-K autoantibody was not associated with smoking, which was believed to be a cause of blood vessel narrowing [31], nor with the presence of anti-U1-RNP and ACAs, which are highly related to MCTD and SSc, respectively [32, 33]. Thus these results suggest that anti-hnRNP-K antibody is particularly relevant to CTD-related secondary RP, but not to a single CTD or primary RP. Our findings should be replicated in a larger study.

The pathogenesis of RP likely involves various abnormalities in the vascular, neural and intravascular systems [4]. At present, it remains to be determined whether anti-hnRNP-K autoantibody detected by our ELISA system can bind to hnRNP-K on vascular endothelial cells *in vivo*. In addition, it is unknown whether this autoantibody contributes to the pathogenesis. Because our cohort of patients includes only a limited number of severe RP patients who experienced hospitalization and/or digit loss, it is unknown whether anti-hnRNP-K antibody correlates with the severity of RP. However, it is tempting to speculate that following cold stimulation, anti-hnRNP-K autoantibody may promote antibody-dependent pathogenesis by inducing vascular endothelial damage. As previously reported, anti-endothelial cell antibodies (AECAs) are a heterogeneous group of autoantibodies against various cell surface proteins in endothelial cells and can contribute leucocyte adhesion by inducing adhesion molecules and cytokines in endothelial cells [34–36]. Anti-hnRNP-K antibody may thus be a class of AECA that becomes active under cold stimulation in patients with secondary RP. Further analyses are needed to elucidate the correlation of anti-hnRNP-K autoantibodies with the pathogenesis of secondary RP.

In summary, we provide the first evidence of cold-associated autoantibodies in patients with secondary RP. Anti-hnRNP-K antibody may be a potential biomarker for RP secondary to CTDs. Longitudinal studies are warranted to determine whether the evaluation of anti-hnRNP-K antibody in RP patients may aid in the detection of CTDs in these patients.

Rheumatology key messages

- Cold-associated autoantibody in patients with secondary RP is successfully identified by a proteomic approach.
- hn-RNP-K translocates to the endothelial cell surface upon cold stimulation.
- Anti-hnRNP-K autoantibody may serve as a biomarker for secondary RP.

Acknowledgements

We would like to thank Y. Kanazawa and J. Yamagishi for secretarial assistance and M. Urase and K. Yoshimoto for technical assistance.

Funding: This study was supported by a grant-in-aid for the Program for Promotion of Fundamental Studies in Health Sciences of the National Institute of Biomedical Innovation and a Grant-in-Aid for Research on Biological Markers for New Drug Development (H20-0005) from the Ministry of Health, Labour and Welfare of Japan.

Disclosure statement: The authors have declared no conflicts of interest.

Supplementary data

Supplementary data are available at *Rheumatology* Online.

References

1 Unwin RD, Griffiths JR, Whetton AD. Simultaneous analysis of relative protein expression levels across multiple samples using iTRAQ isobaric tags with 2D nano LC-MS/MS. Nat Protoc 2010;5:1574–82.

2 Serada S, Fujimoto M, Ogata A *et al*. iTRAQ-based proteomic identification of leucine-rich alpha-2 glycoprotein as a novel inflammatory biomarker in autoimmune diseases. Ann Rheum Dis 2010;69:770–4.

3 Yokoyama T, Enomoto T, Serada S *et al*. Plasma membrane proteomics identifies bone marrow stromal antigen 2 as a potential therapeutic target in endometrial cancer. Int J Cancer 2013;132:472–84.

4 Herrick AL. The pathogenesis, diagnosis and treatment of Raynaud phenomenon. Nat Rev Rheumatol 2012;8:469–79.

5 Bakst R, Merola JF, Franks AG Jr, Sanchez M. Raynaud's phenomenon: pathogenesis and management. J Am Acad Dermatol 2008;59:633–53.

6 Dimant J, Ginzler E, Schlesinger M *et al*. The clinical significance of Raynaud's phenomenon in systemic lupus erythematosus. Arthritis Rheum 1979;22:815–9.

7 Grader-Beck T, Wigley FM. Raynaud's phenomenon in mixed connective tissue disease. Rheum Dis Clin North Am 2005;31:465–81, vi.

8 Maricq HR, Harper FE, Khan MM, Tan EM, LeRoy EC. Microvascular abnormalities as possible predictors of disease subsets in Raynaud phenomenon and early connective tissue disease. Clin Exp Rheumatol 1983;1:195–205.

9 Srivastava R, Aslam M, Kalluri SR *et al*. Potassium channel KIR4.1 as an immune target in multiple sclerosis. N Engl J Med 2012;367:115–23.

10 Serada S, Fujimoto M, Takahashi T *et al*. Proteomic analysis of autoantigens associated with systemic lupus erythematosus: anti-aldolase A antibody as a potential marker of lupus nephritis. Proteomics Clin Appl 2007;1:185–91.

11 He P, Naka T, Serada S *et al*. Proteomics-based identification of alpha-enolase as a tumor antigen in non-small lung cancer. Cancer Sci 2007;98:1234–40.

12 Masi AT. Preliminary criteria for the classification of systemic sclerosis (scleroderma). Subcommittee for scleroderma criteria of the American Rheumatism Association Diagnostic and Therapeutic Criteria Committee. Arthritis Rheum 1980;23:581–90.

13 Tan EM, Cohen AS, Fries JF *et al*. The 1982 revised criteria for the classification of systemic lupus erythematosus. Arthritis Rheum 1982;25:1271–7.

14 Hochberg MC. Updating the American College of Rheumatology revised criteria for the classification of systemic lupus erythematosus. Arthritis Rheum 1997;40:1725.

15 Kasukawa R, Tojo T, Miyawaki S. Preliminary diagnostic criteria for classification of mixed connective tissue disease. In: Kasukawa R, Sharp GC, eds. Mixed Connective Tissue Diseases and Antinuclear Antibodies. Amsterdam, the Netherlands: Elsevier, 1987:41–7.

16 Brennan P, Silman A, Black C *et al*. Validity and reliability of three methods used in the diagnosis of Raynaud's phenomenon. The UK Scleroderma Study Group. Br J Rheumatol 1993;32:357–61.

17 Umegaki-Arao N, Tamai K, Nimura K *et al*. Karyopherin alpha2 is essential for rRNA transcription and protein synthesis in proliferative keratinocytes. PLoS One 2013;8:e76416.

18 Yang L, Serada S, Fujimoto M *et al*. Periostin facilitates skin sclerosis via PI3K/Akt dependent mechanism in a mouse model of scleroderma. PLoS One 2012;7:e41994.

19 Han SP, Tang YH, Smith R. Functional diversity of the hnRNPs: past, present and perspectives. Biochem J 2010;430:379–92.

20 Dreyfuss G, Matunis MJ, Pinol-Roma S, Burd CG. hnRNP proteins and the biogenesis of mRNA. Annu Rev Biochem 1993;62:289–321.

21 Furukawa F, Kashihara-Sawami M, Lyons MB, Norris DA. Binding of antibodies to the extractable nuclear antigens SS-A/Ro and SS-B/La is induced on the surface of human keratinocytes by ultraviolet light (UVL): implications for the pathogenesis of photosensitive cutaneous lupus. J Invest Dermatol 1990;94:77–85.

22 Wang B, Dong X, Yuan Z, Zuo Y, Wang J. SSA/Ro antigen expressed on membrane of UVB-induced apoptotic keratinocytes is pathogenic but not detectable in supernatant of cell culture. Chin Med J 1999;112:512–5.

23 Golan TD, Elkon KB, Gharavi AE, Krueger JG. Enhanced membrane binding of autoantibodies to cultured keratinocytes of systemic lupus erythematosus patients after ultraviolet B/ultraviolet A irradiation. J Clin Invest 1992;90:1067–76.

24 Nickel W, Seedorf M. Unconventional mechanisms of protein transport to the cell surface of eukaryotic cells. Annu Rev Cell Dev Biol 2008;24:287–308.

25 Nickel W, Rabouille C. Mechanisms of regulated unconventional protein secretion. Nat Rev Mol Cell Biol 2009;10:148–55.

26 Nickel W. Pathways of unconventional protein secretion. Curr Opin Biotechnol 2010;21:621–6.

27 Bomsztyk K, Denisenko O, Ostrowski J. hnRNP K: one protein multiple processes. Bioessays 2004;26:629–38.

28 Qi Z, Takamatsu H, Espinoza JL *et al*. Autoantibodies specific to hnRNP K: a new diagnostic marker for immune pathophysiology in aplastic anemia. Ann Hematol 2010;89:1255–63.

29 Van den Bergh K, Hooijkaas H, Blockmans D *et al*. Heterogeneous nuclear ribonucleoprotein h1, a novel nuclear autoantigen. Clin Chem 2009;55:946–54.

30 Op De Beeck K, Maes L, Van den Bergh K *et al*. Heterogeneous nuclear RNPs as targets of autoantibodies in systemic rheumatic diseases. Arthritis Rheum 2012;64:213–21.

31 D.S.G. Tobacco report: PHS Study Group, after 14-month survey, agrees that smoking is indeed harmful. Science 1964;143:227.

32 Buchanan RR, Riglar AG. The titre of anti-centromere antibodies: its relationship to Raynaud's phenomenon and vascular occlusion. Br J Rheumatol 1989;28:221–6.

33 Furtado RN, Pucinelli ML, Cristo VV, Andrade LE, Sato EI. Scleroderma-like nailfold capillaroscopic abnormalities are associated with anti-U1-RNP antibodies and Raynaud's phenomenon in SLE patients. Lupus 2002;11: 35–41.

34 Carvalho D, Savage CO, Black CM, Pearson JD. IgG antiendothelial cell autoantibodies from scleroderma patients induce leukocyte adhesion to human vascular endothelial cells in vitro. Induction of adhesion molecule expression and involvement of endothelium-derived cytokines. J Clin Invest 1996;97:111–9.

35 Del Papa N, Guidali L, Sironi M *et al*. Anti-endothelial cell IgG antibodies from patients with Wegener's granulomatosis bind to human endothelial cells in vitro and induce adhesion molecule expression and cytokine secretion. Arthritis Rheum 1996;39:758–66.

36 Lin CF, Chiu SC, Hsiao YL *et al*. Expression of cytokine, chemokine, and adhesion molecules during endothelial cell activation induced by antibodies against dengue virus nonstructural protein 1. J Immunol 2005;174:395–403.

Journal of General Virology (2014), 95, 2769–2777 DOI 10.1099/vir.0.069336-0

Human herpesvirus 6 gM/gN complex interacts with v-SNARE in infected cells

Akiko Kawabata,[1] Satoshi Serada,[2] Tetsuji Naka[2] and Yasuko Mori[1]

Correspondence
Yasuko Mori
ymori@med.kobe-u.ac.jp

[1]Division of Clinical Virology, Center for Infectious Diseases, Kobe University Graduate School of Medicine, 7-5-1, Kusunoki-cho, Chuo-ku, Kobe 650-0017, Japan

[2]Laboratory of Immune Signal, Division of Biomedical Research, National Institute of Biomedical Innovation, 7-6-8, Saito-Asagi, Ibaraki, Osaka 567-0085, Japan

Human herpesvirus 6 (HHV-6) glycoprotein M (gM) is an envelope glycoprotein that associates with glycoprotein N (gN), forming the gM/gN protein complex, in a similar manner to the other herpesviruses. Liquid chromatography-MS/MS analysis showed that the HHV-6 gM/gN complex interacts with the v-SNARE protein, vesicle-associated membrane protein 3 (VAMP3). VAMP3 colocalized with the gM/gN complex at the *trans*-Golgi network and other compartments, possibly the late endosome in HHV-6-infected cells, and its expression gradually increased during the late phase of virus infection. Finally, VAMP3 was incorporated into mature virions and may be transported with the gM/gN complex.

Received 23 June 2014
Accepted 9 September 2014

INTRODUCTION

Human herpesvirus 6 (HHV-6) belongs to the betaherpesvirus subfamily (Roizmann *et al.*, 1992). HHV-6 isolates can be classified as HHV-6A and HHV-6B (Ablashi *et al.*, 2013) based on genetic and antigenic differences, cell tropism, and pathogenesis (Ablashi *et al.*, 1991; Aubin *et al.*, 1991; Campadelli-Fiume *et al.*, 1993; Chandran *et al.*, 1992; Mori, 2009; Yamanishi *et al.*, 1988).

Herpesviruses encode several glycoproteins on the envelope of viral particles that work for entry, assembly and egress of the virus. Of these, glycoprotein M (gM) is a remarkable envelope glycoprotein as it is conserved among all herpesvirus subfamilies. Most herpesviruses, including herpes simplex virus type-1 (Baines & Roizman, 1991), pseudorabies virus (Dijkstra *et al.*, 1996) and equine herpesvirus 1 (Osterrieder *et al.*, 1996), do not require gM for replication. Marek's disease virus (Tischer *et al.*, 2002) and varicella-zoster virus (Yamagishi *et al.*, 2008) abolish virus growth *in vitro*. However, the gM protein of human cytomegalovirus (HCMV), which belongs to the betaherpesvirus subfamily, is essential for the production of infectious virus (Hobom *et al.*, 2000).

HHV-6 gM is a product of the U72 ORF and comprises 343 aa (Kawabata *et al.*, 2012; Lawrence *et al.*, 1995). Post-infection (p.i.), it is translated into a 47–63 kDa protein that is post-translationally glycosylated (Kawabata *et al.*, 2012). It is a type III transmembrane protein with seven membrane-spanning domains and a C-terminal cytoplasmic tail. HHV-6 gM interacts with the product of the U46 ORF, known as gN, to form a complex for transport to the *trans*-Golgi network (TGN) and endosomal compartments (Kawabata *et al.*, 2012). Finally, the gM/gN complex is incorporated into mature virions. Interestingly, unlike in alpha herpesviruses, HHV-6 gM is essential for virus growth (Kawabata *et al.*, 2012).

To further examine the role of HHV-6A gM during HHV-6 infection, we performed liquid chromatography (LC)-MS/MS analysis to identify the cellular components that interact with the gM/gN complex. The results showed that the gM/gN complex interacts with VAMP3 (vesicle-associated membrane protein 3).

VAMP3 is a v-SNARE (soluble *N*-ethylmaleimide-sensitive factor attachment protein receptor) protein that resides in recycling endosomes and endosome-derived transport vesicles. v-SNARE interacts with SNARE proteins on target membranes (t-SNAREs) to form *trans*-SNARE complexes, which draw the two membranes together and drive membrane fusion (Jahn & Scheller, 2006; Jahn *et al.*, 2003; Rothman, 1994; Söllner *et al.*, 1993). SNAREs are cytoplasmic-oriented type I membrane proteins that play a role in intracellular trafficking mechanisms during exocytosis by forming a complex that facilitates the transient fusion of the vesicular and plasma membrane lipid bilayers (Mohrmann & Sørensen, 2012). This membrane fusion is dependent on the formation of a complex between t-SNARE and v-SNARE proteins (Jahn & Scheller, 2006; Jahn *et al.*, 2003).

VAMP3 is localized to recycling endosomes (McMahon *et al.*, 1993) and plays a role in the fusion of recycling endosomes and the plasma membrane by forming a complex with the surface t-SNARE complex, Stx4/SNAP23 (Hu *et al.*, 2007). The VAMP3/Stx4/SNAP23 SNARE complex mediates the long-loop recycling pathway that delivers recycling endosomes and their cargo to the cell

surface, and plays an important role in regulating the ability of macrophages to effectively adhere and spread on fibronectin (Veale *et al.*, 2011). VAMP3 is also involved in integrin trafficking, cell migration and cell adhesion (Luftman *et al.*, 2009; Tayeb *et al.*, 2005). In addition, it plays a role in the exocytosis of α-granules in platelets (Polgár *et al.*, 2002), as well as in the recycling of endocytosed transferrin receptors to the cell surface (Galli *et al.*, 1994).

Here, we describe the interaction between the gM/gN complex and VAMP3 in HHV-6A-infected cells and discuss the potential for the association between the gM/gN complex and VAMP3 to modify its localization and mediate its incorporation into mature virions.

RESULTS

Identification of cellular proteins interacting with the gM/gN complex

A recent study showed that the cytoplasmic tail of HCMV gM interacts with the cellular protein FIP4, which is a Rab11-GTPase effector protein important for gM/gN trafficking and for accumulation of the envelope glycoprotein complex in the assembly compartment in HCMV-infected cells (Krzyzaniak *et al.*, 2009). To examine the function of HHV-6A gM/gN, we tried to identify the cellular protein(s) that interact with the gM/gN complex. First, gM and gN were cotransfected into 293T cells and gM was immunoprecipitated from the lysates with an anti-gM mAb. Silver staining of gels containing proteins separated from the lysates of the gM/gN-expressing cells revealed several specific bands at approximately 10 kDa; these proteins were not present in the lysates of cells expressing gM alone. One specific band (Fig. 1a, arrowhead) was excised from the gel and subjected to LC-MS/MS analysis. The results of this analysis identified VAMP3 as the interacting protein (Fig. 1b).

To confirm the interaction between VAMP3 and gM/gN, lysates from cells expressing both HA-tagged gM and FLAG-tagged gN were immunoprecipitated with an anti-HA antibody, followed by Western blotting with anti-gM, anti-FLAG or anti-VAMP3 antibodies. As shown in Fig. 1c, VAMP3 was coprecipitated when gM and gN were coexpressed. However, VAMP3 was not coprecipitated when gM or gN was expressed alone. CD63 was not coprecipitated even when gM and gN were coexpressed (Fig. 1c). These results indicate that VAMP3 interacts with the gM/gN complex.

Interaction between gM and VAMP3 in HHV-6A-infected cells

To confirm the interaction between the gM/gN complex and VAMP3 in HHV-6A-infected cells, lysates from HHV-6A-infected HSB-2 cells were immunoprecipitated with an anti-gM mAb or an anti-VAMP3 antibody, followed by Western blotting with anti-gM, anti-VAMP3, anti-CD63 or anti-gB antibodies (Fig. 2). Endogenous VAMP3 coprecipitated with gM and vice versa; gB or endogenous CD63 coprecipitated with neither gM nor VAMP3 (Fig. 2b). These results indicate that gM also interacts with VAMP3 in HHV-6A-infected cells. Interestingly, although gM with a molecular mass of 15 kDa was detected in the lysates of HHV-6A-infected cells, it did not coprecipitate with the anti-VAMP3 antibody.

To examine the cellular localization of gM and VAMP3 in HHV-6A-infected cells, an indirect immunofluorescence assay (IFA) was performed using HHV-6A-infected HSB-2 cells at 96 h p.i. (Fig. 3). Confocal microscopy of HHV-6A-infected HSB-2 cells showed that gM and VAMP3 appear to partially colocalize to the same cellular compartment. In addition, gM and VAMP3 partially colocalized with TGN46, a marker of the TGN (Fig. 3b), and with CD63, a marker of late endosomes and multivesicular bodies (MVB) (Fig. 3a). The expression of endogenous VAMP3 was much lower in uninfected cells than infected cells [Fig. 3a(ii), b(ii)]. These results indicate that VAMP3 may localize with gM to the endosomal compartment in addition to TGN during the late stage of infection. Preimmune serum of guinea pig did not react with either HHV-6A-infected [Fig. 3d(i)] or uninfected cells [Fig. 3d(ii)], although anti-VAMP3 antibody obtained from the same guinea pig reacted with HHV-6A-infected cells [Fig. 3c(i)] but not uninfected cells [Fig. 3c(ii)].

VAMP3 is present in purified HHV-6A virions

Recently, we showed that HHV-6A virions are released through MVBs via the cellular exosomal pathway and that gB and gM are present on exosomes (Mori *et al.*, 2008). To examine whether VAMP3 expressed in HHV-6A-infected cells is present on virions and exosomes, we purified virions from the culture medium of HHV-6A-infected cells. As expected, VAMP3, gM and CD63 were detected by western blotting of the virion fractions (Fig. 4a). Virion fractions were confirmed with the presence of gB (Fig. 4a) and viral DNA (Fig. 4b). In addition, VAMP3 was detected on HHV-6A virions by immunogold labelling electron microscopy analysis [Fig. 4c(i)], but it was rarely detected on virions without primary antibody [Fig. 4c(ii)]. These results indicate that VAMP3 is incorporated into viral particles along with the gM/gN complex.

Intracellular localization of the gM/gN complex and VAMP3 in cells transiently expressing gM/gN

We next examined the intracellular localization of gM, gN and VAMP3 (Fig. 5). When plasmids expressing gM and gN were cotransfected into HeLa cells [Fig. 5a(i)], gM/gN colocalized with endogenous VAMP3 in the perinuclear region. However, when gM was expressed alone, it failed to colocalize with VAMP3 [Fig. 5a(ii)]. Because the gM/gN complex localized to the TGN in HHV-6A-infected cells, we hypothesized that the gM/gN complex would interact with

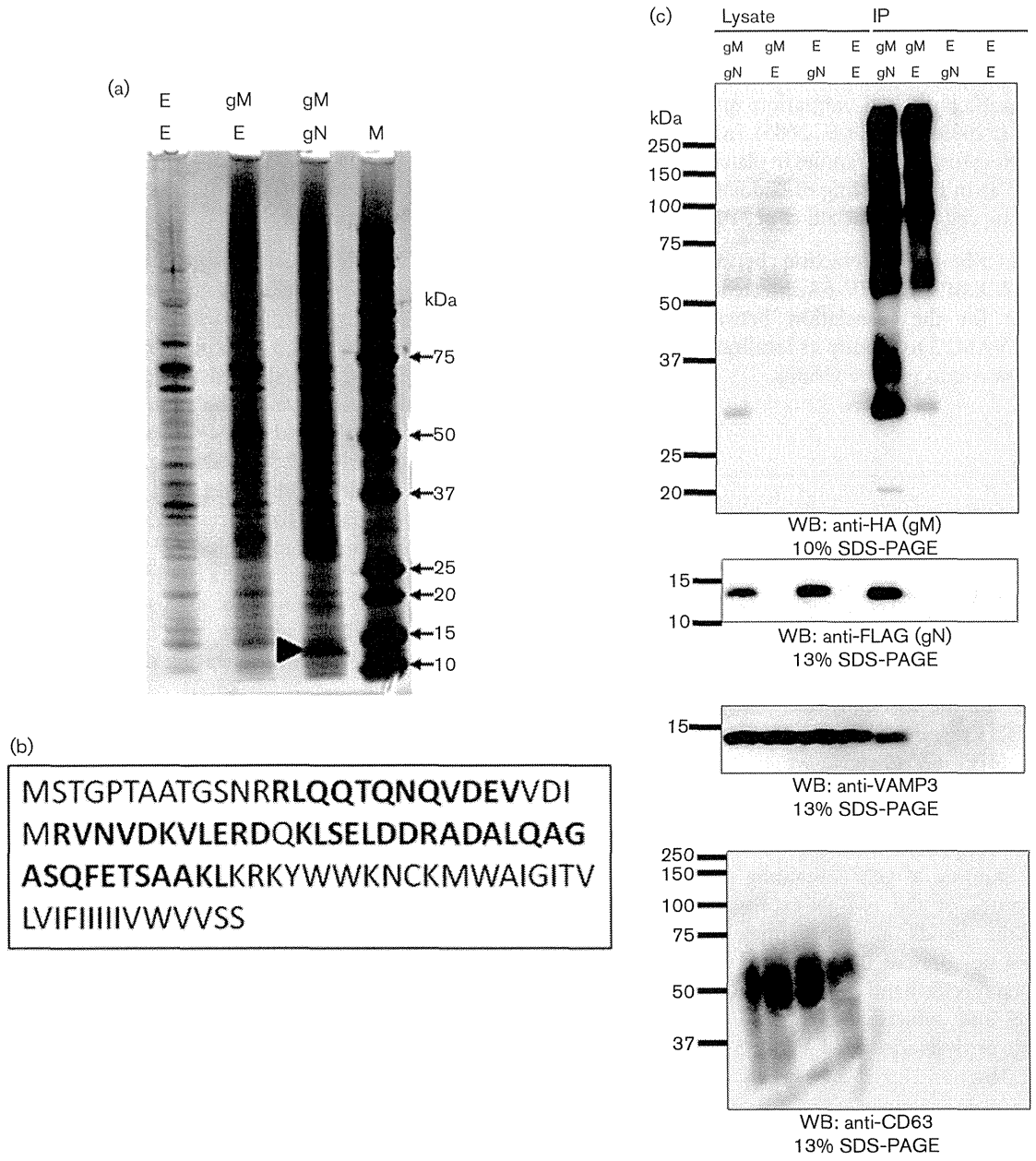

Fig. 1. Interaction between gM/gN and VAMP3. (a) 293T cells were transfected with plasmids expressing HA-tagged gM and FLAG-tagged gN. The cells were lysed with TNE buffer at 72 h post-transfection. The lysates were then immunoprecipitated with an anti-HA Ab specific for gM and visualized by silver staining. The band marked by the arrowhead indicates the protein selected for analysis by LC-MS/MS. (b) Peptide matches to the VAMP3 sequence are shown in bold. (c) 293T cells were transfected with plasmids expressing HA-tagged gM, FLAG-tagged gN, or pCAGGS (negative control). The cells were then lysed with TNE buffer at 72 h post-transfection. The lysates were immunoprecipitated with anti-HA antibody for gM and analysed by Western blotting with anti-HA, anti-FLAG, anti-VAMP3 (BioReagents) or anti-CD63 antibodies. The numbers beside the panels indicate the molecular masses (kDa). WB, Western blotting; E, empty.

VAMP3 at the TGN or a TGN-derived compartment. As expected, when gM was coexpressed with gN, it colocalized with VAMP3 and TGN46 (Fig. 5b); however, this colocalization was not observed when gM was expressed alone [Fig. 5a(ii)]. These results suggest that the interaction between the gM/gN complex and VAMP3 occurs at the TGN or a TGN-derived compartment. Glycoprotein M did not colocalize with CD63 even when gM was coexpressed with gN [Fig. 4c(i)]. Non-specific staining of gM was not seen in these cells [Fig. 5a(iii), b(ii), c(ii)].

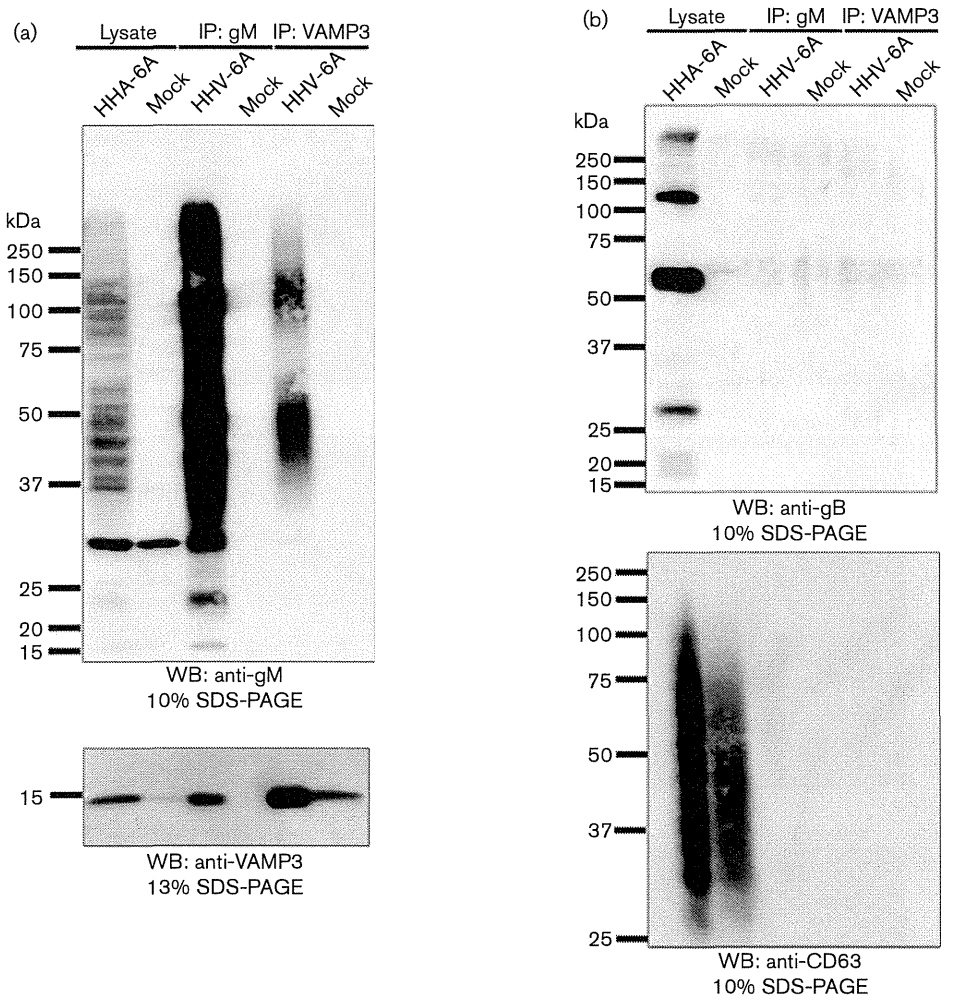

Fig. 2. Interaction between gM and VAMP3 in HHV-6A-infected HSB-2 cells. HHV-6A-infected or mock-infected HSB-2 cells were lysed with TNE buffer at 96 h post-infection. The lysates were immunoprecipitated (IP) with anti-gM mAb or anti-VAMP3 Ab (see Methods) and analysed by Western blotting with anti-gM or anti-VAMP3 (BioReagents) Abs (a), anti-gB Ab or anti-CD63 mAb (b). The numbers beside the panels indicate the molecular masses (kDa). WB, Western blotting.

The kinetics of VAMP3 expression in HHV-6A-infected cells

As shown in Fig. 2, VAMP3 expression in HHV-6A-infected cells was higher than that in mock-infected cells. Therefore, we examined the kinetics of VAMP3 expression in HHV-6A-infected cells. The results in Fig. 6 show that VAMP3 expression increased gradually in the infected cells.

DISCUSSION

Here, we used the transient expression of gM and gN to identify VAMP3 as a cellular molecule that interacts with the HHV-6A gM/gN complex. The interaction between VAMP3 and the gM/gN complex was also confirmed in HHV-6A-infected cells. VAMP3 and gM/gN proteins colocalized at the TGN in cells coexpressing gM and gN, and in HHV-6A-infected cells. This interaction was observed only when gM/gN formed a complex, indicating that the interaction is required for gM/gN complex formation. Previously, we reported that the localization of HHV-6A gM to the TGN was necessary for its interaction with gN (Kawabata *et al.*, 2012). Therefore, the interaction between the gM/gN complex and VAMP3 might also occur at the TGN. It is still not known whether the interaction between VAMP3 and gM requires gM/gN complex formation. Transport of gM to the TGN might be required for this interaction.

VAMP3 also colocalized with CD63, which is a marker of late endosome in HHV-6A-infected cells. In cells transiently expressing gM and gN, however, VAMP3 colocalized with TGN46, but not CD63. This suggests that in infected cells, the localization of VAMP3 may be modified through its interaction with gM/gN, thereby possibly allowing it to localize to the other organelles, such as the late endosome.

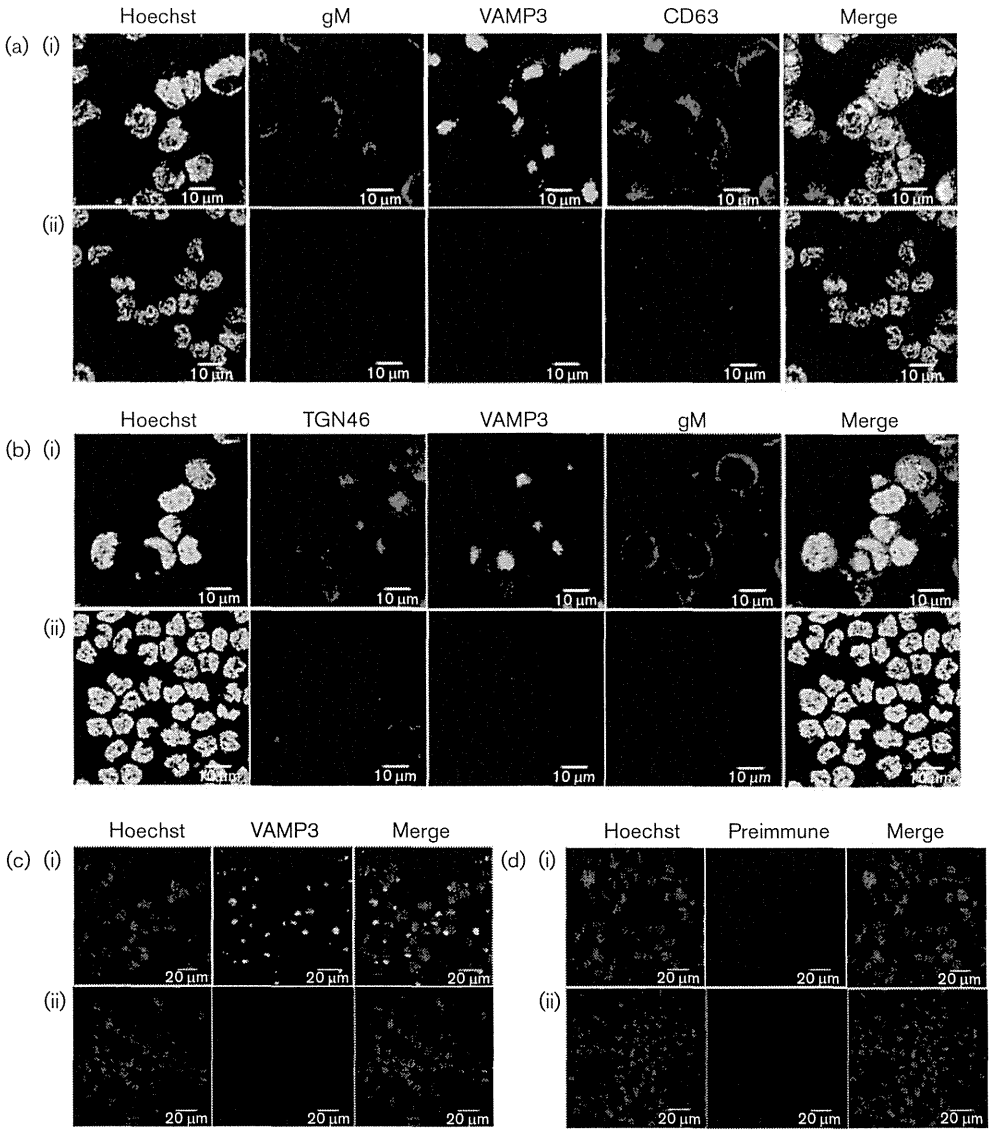

Fig. 3. Colocalization of gM, VAMP3 and CD63, or gM, VAMP3 and TGN46 in HHV-6A-infected cells. HHV-6A-infected [a(i), b(i)] or mock-infected [a(ii), b(ii)] HSB-2 cells were harvested at 96 h post-infection and fixed. The cells were stained with antibodies against VAMP3, gM and CD63 as well as with Hoechst 33258 (a), or VAMP3, gM and TGN46 as well as with Hoechst 33258 (b). Costained areas appear white in the merged panel. Bars, 10 μm. HHV-6A-infected [c(i), d(i)] or mock-infected [c(ii), d(ii)] cells were stained with guinea pig antisera against VAMP3 (c) or preimmune sera obtained from the same guinea pig as well as with Hoechst 33258 (d). Bars, 20 μm.

We also found that VAMP3 was incorporated into virions. As the gM/gN complex is expressed on virions and exosomes, complex-associated VAMP3 would be transported along with the gM/gN complex and then released via the exosomal release pathway (Mori *et al.*, 2008).

Although the function of VAMP3 in HHV-6A-infected cells is not known, its interaction with the gM/gN complex may modify the cellular machinery in infected cells. As VAMP3 is incorporated into virions and exosomes, its primary function (to facilitate membrane fusion) may be lost in infected cells. Overexpression of VAMP3 did not affect HHV-6 growth (data not shown). Several v-SNARE proteins with functions similar to those of VAMP3 have been identified (Borisovska *et al.*, 2005). Therefore, the function of VAMP3 may be redundant in HHV-6A-infected cells. It is still not known whether v-SNAREs, including VAMP3, are required for HHV-6 infection. Further studies will be required to address these questions.

METHODS

Cells and viruses. The HSB-2 T-cell line was cultured in RPMI 1640 medium (Nissui) supplemented with 8% FBS. Human embryonic

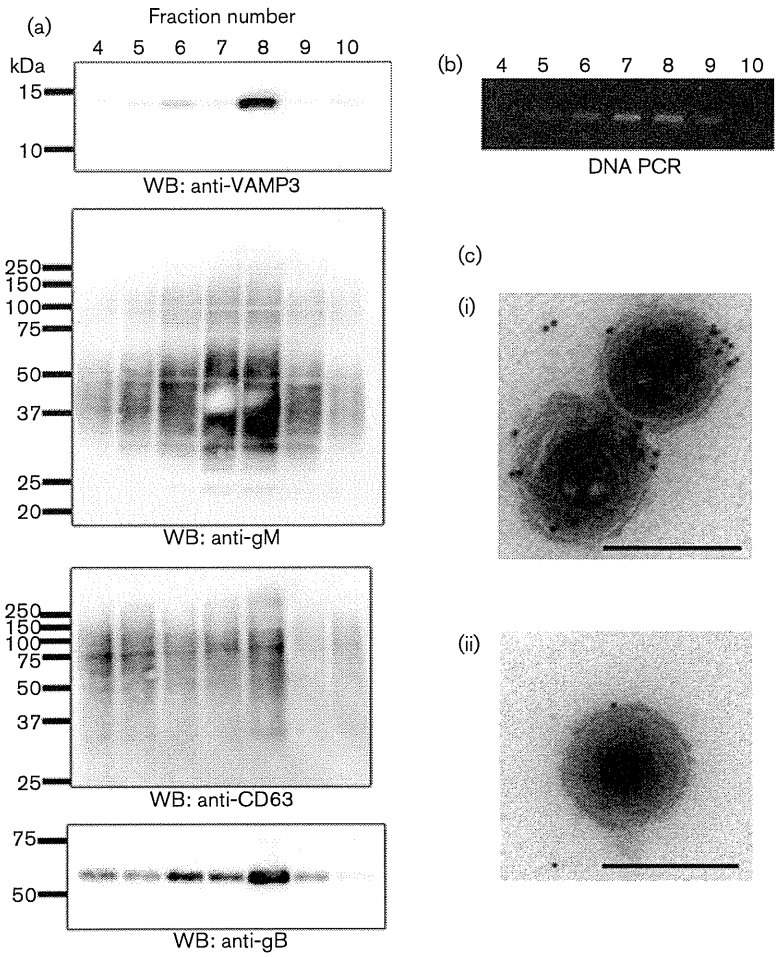

Fig. 4. The presence of VAMP3 in HHV-6A virions and exosomes. Exosome fractions containing virions were purified from the culture medium of HHV-6A-infected cells by sucrose density-gradient centrifugation and then analysed by Western blotting (a), DNA PCR (b) and electron microscopy (c). (a) Western blot analysis of the sucrose density-gradient fractions with anti-VAMP3, anti-gM, anti-CD63 or anti-gB Abs. (b) Viral DNA was detected in the fractions by PCR with HHV-6A specific primers. The numbers above the PCR image showed the fraction numbers. (c) Immunogold localization of VAMP3 on the HHV-6A virions. Purified virions (fraction 8) were labelled with antisera against VAMP3 (i) or without primary antibody (ii). Bars, 200 nm.

kidney cells (293T cells) and HeLa cells were cultured in Dulbecco's modified Eagle's medium supplemented with 8 % FBS. The HHV-6A strain GS was propagated and titrated in HSB-2 cells. HHV-6A cell-free virus was prepared as previously described (Akkapaiboon *et al.*, 2004). Cord blood mononuclear cells (CBMC) were used for virus propagation (Mori *et al.*, 2004). CBMCs were kindly provided by K. Adachi (Minoh Hospital, Minoh, Japan) and H. Yamada (Kobe University Graduate School of Medicine, Kobe, Japan) and purchased from the RIKEN Cell Bank (BioResource Center). For the usage of CBMCs, the study was approved by the ethics committee of each institution.

Antibodies. Rabbit antibody (Ab) specific for HHV-6A gM or gB (Mori *et al.*, 2008), an AgM-1 mAb against gM (Kawabata *et al.*, 2012), and a U14 mAb against HHV-6 U14 (Takemoto *et al.*, 2005) were used. mAbs against CD63 (clone CLB-gran/12, 435; Sanquin) and α-tubulin (clone B-5-1-2; Sigma), a sheep polyclonal Ab against TGN46 (AbD Serotec), a rabbit polyclonal Ab against VAMP3 (BioReagents) and a goat polyclonal Ab against VAMP3 (Santa Cruz) were used. Anti-HA (clone HA-7; Sigma) and anti-FLAG (clone M2; Sigma) antibodies were also used. Alexa Fluor 594-conjugated donkey anti-sheep IgG (Molecular Probes), Alexa Fluor 594-conjugated donkey anti-rabbit IgG (Molecular Probes), FITC-conjugated affinity pure $F(ab')_2$ fragment goat anti-guinea pig IgG (Jackson ImmunoResearch Laboratories), and Cy5-conjugated donkey anti-mouse IgG (Jackson ImmunoResearch Laboratories) were used as secondary antibodies. An anti-VAMP3 monospecific Ab was produced by subjecting guinea pigs to three rounds of immunization with the antigen, which was then expressed in *Escherichia coli* and purified (Mori *et al.*, 2008).

Immunofluorescence assay. The IFA was performed as described previously (Akkapaiboon *et al.*, 2004; Mori *et al.*, 2004). Specific immunofluorescence was observed under a confocal laser-scanning microscope (FluoView FV1000; Olympus).

Plasmid construction. The HA-tagged gM- and FLAG-tagged gN-expressing plasmids were described previously (Kawabata *et al.*, 2012). The pCAGGS plasmid was kindly provided by Jun-ichi Miyazaki (Osaka University, Japan) (Niwa *et al.*, 1991). To express the recombinant protein, the following primer pair was used to amplify inserts from HSB-2 cells cDNA: for named GST-VAMP3, VAMP3FbamHI (5′-ACCGGATCCTCTACAGGTCCAACTGCTGC-CACT-3′) and VAMP3rsalI (5′-ACCGTCGACTTACTTGCAATTCT-TCCACCAATATTTC-3′). The PCR products were inserted into the pGEX-4T1 vector (GE Healthcare).

Plasmid transfection. HeLa cells were transfected with the expression plasmids using Lipofectamine 2000 (Invitrogen) according to the manufacturer's instructions. The 293T cells were transfected using the calcium phosphate method as described previously (Koshizuka *et al.*, 2010).

Identification of gM/gN-interacting proteins. Plasmids expressing HA-tagged gM and FLAG-tagged gN were cotransfected into 293T cells. Cotransfection of gM and pCAGGS into 293T cells was performed as a control. At 72 h post-transfection, the cells were lysed in TNE buffer (0.01 M Tris/HCl, pH 7.4, 0.15 M NaCl, 1 mM EDTA, 1 % Nonidet-P-40). After centrifugation at 200 000 *g* for 1 h, the

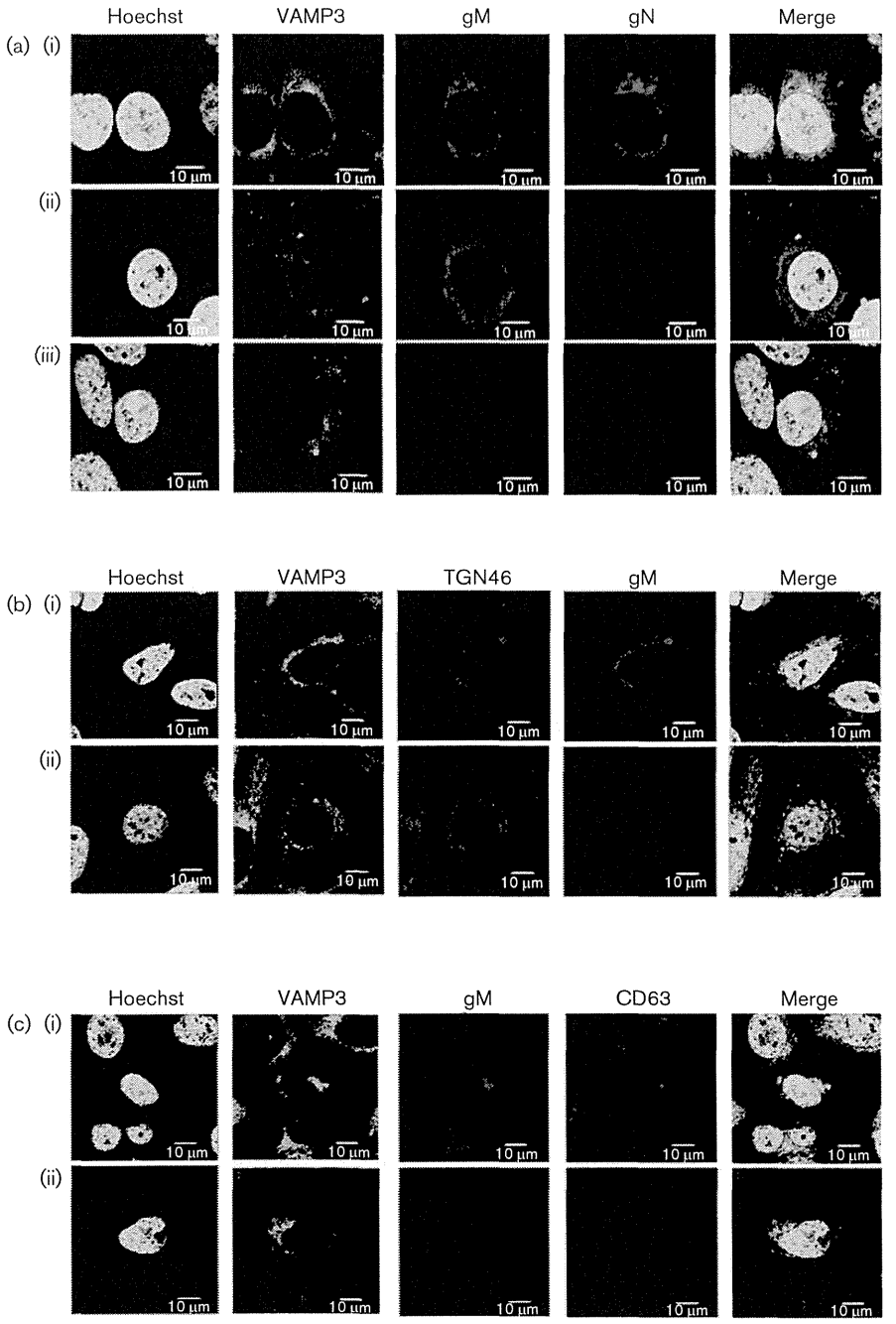

Fig. 5. Subcellular localization of VAMP3 with the gM/gN complex in HeLa cells transiently expressing gM and gN. HeLa cells were transfected with plasmids expressing gM and gN [a(i), b(i), c(i)], gM and the empty vector [a(ii)], or without vectors [a(iii), b(ii), c(ii)]. The cells were harvested at 48 h post-transfection and fixed. (a) The cells were stained with antibodies against gM, FLAG (for gN) and VAMP3 as well as with Hoechst 33258. (b) Cells were stained with antibodies against gM, TGN46 and VAMP3 as well as Hoechst 33258. (c) Cells were stained with antibodies against gM, CD63 and VAMP3 as well as with Hoechst 33258. Co-stained areas appear white or yellow in the merged panel. Bars, 10 μm.

supernatants were incubated overnight at 4 °C with an anti-HA antibody conjugated to protein G Sepharose (GE Healthcare). The protein-anti-HA conjugated beads were then washed with lysis buffer and the bound proteins were eluted with 0.1 M glycine/HCl (pH 2.8). After the beads were removed by centrifugation, the supernatants were neutralized by adding 1 M Tris-HCl (pH 9.5). The eluted proteins were then solubilized with sample buffer, separated on a NuPAGE SDS-PAGE system (Invitrogen), and examined by silver staining. Specific bands were analysed by LC-MS/MS to identify the coimmunoprecipitated proteins (Shevchenko *et al.*, 1996; Tang *et al.*, 2013).

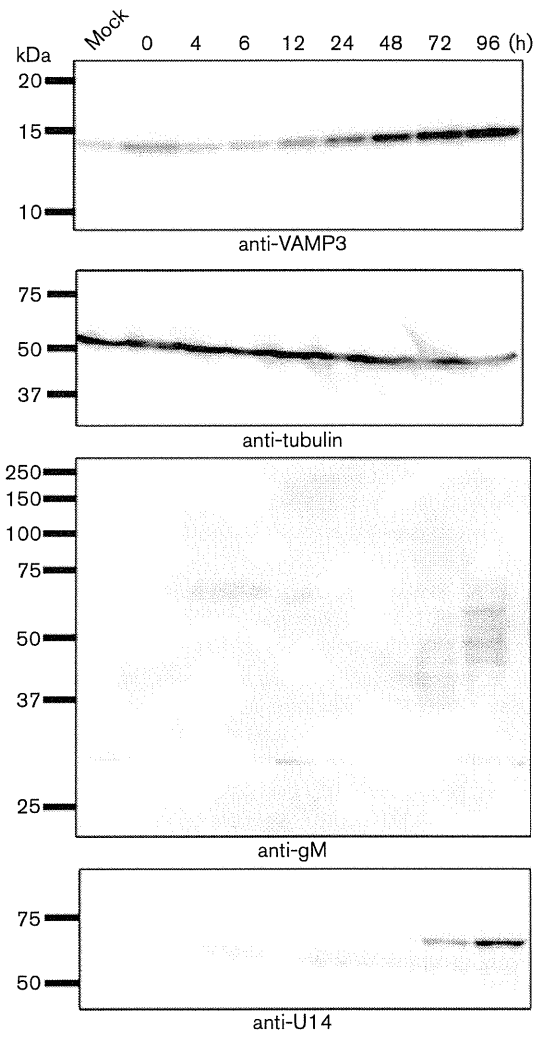

Fig. 6. Kinetics of VAMP3 protein expression in HHV-6A-infected cells. Whole-cell lysates collected at the indicated time points (h) were analysed by Western blotting. The numbers beside the panels indicate the molecular masses (kDa).

Western blotting. Western blotting was performed as described previously (Akkapaiboon *et al.*, 2004).

Isolation of virion fractions. Virions containing exosomes were collected from the cell culture medium by differential centrifugation and fractionated with a linear sucrose gradient, as described previously (Mori *et al.*, 2008). The fractions were analysed by Western blotting, DNA PCR, and electron microscopy.

Electron microscopy. Immunogold labelling of virions was performed as described previously (Mori *et al.*, 2008). The samples were examined under a Hitachi H-7650 electron microscope.

ACKNOWLEDGEMENTS

We thank E. Moriishi (National Institute of Biomedical Innovation), Mayuko Hayashi and Megumi Ota (Kobe University) for technical assistance, J. Miyazaki (Osaka University) for providing reagents, and K. Adachi (Minoh City Hospital) and H. Yamada (Kobe University) for the CBMCs. This work was supported by a Grant-in-Aid for Scientific Research (B) from the Japan Society for the Promotion of Science (JSPS).

REFERENCES

Ablashi, D. V., Balachandran, N., Josephs, S. F., Hung, C. L., Krueger, G. R., Kramarsky, B., Salahuddin, S. Z. & Gallo, R. C. (1991). Genomic polymorphism, growth properties, and immunologic variations in human herpesvirus-6 isolates. *Virology* **184**, 545–552.

Ablashi, D., Agut, H., Alvarez-Lafuente, R., Clark, D. A., Dewhurst, S., Diluca, D., Flamand, L., Frenkel, N., Gallo, R. & other authors (2014). Classification of HHV-6A and HHV-6B as distinct viruses. *Arch Virol* **159**, 863–870.

Akkapaiboon, P., Mori, Y., Sadaoka, T., Yonemoto, S. & Yamanishi, K. (2004). Intracellular processing of human herpesvirus 6 glycoproteins Q1 and Q2 into tetrameric complexes expressed on the viral envelope. *J Virol* **78**, 7969–7983.

Aubin, J. T., Collandre, H., Candotti, D., Ingrand, D., Rouzioux, C., Burgard, M., Richard, S., Huraux, J. M. & Agut, H. (1991). Several groups among human herpesvirus 6 strains can be distinguished by Southern blotting and polymerase chain reaction. *J Clin Microbiol* **29**, 367–372.

Baines, J. D. & Roizman, B. (1991). The open reading frames UL3, UL4, UL10, and UL16 are dispensable for the replication of herpes simplex virus 1 in cell culture. *J Virol* **65**, 938–944.

Borisovska, M., Zhao, Y., Tsytsyura, Y., Glyvuk, N., Takamori, S., Matti, U., Rettig, J., Südhof, T. & Bruns, D. (2005). v-SNAREs control exocytosis of vesicles from priming to fusion. *EMBO J* **24**, 2114–2126.

Campadelli-Fiume, G., Guerrini, S., Xiaoming, L. & Foà-Tomasi, L. (1993). Monoclonal antibodies to glycoprotein B differentiate human herpesvirus 6 into two clusters, variants A and B. *J Gen Virol* **74**, 2257–2262.

Chandran, B., Tirawatnapong, S., Pfeiffer, B. & Ablashi, D. V. (1992). Antigenic relationships among human herpesvirus-6 isolates. *J Med Virol* **37**, 247–254.

Dijkstra, J. M., Visser, N., Mettenleiter, T. C. & Klupp, B. G. (1996). Identification and characterization of pseudorabies virus glycoprotein gM as a nonessential virion component. *J Virol* **70**, 5684–5688.

Galli, T., Chilcote, T., Mundigl, O., Binz, T., Niemann, H. & De Camilli, P. (1994). Tetanus toxin-mediated cleavage of cellubrevin impairs exocytosis of transferrin receptor-containing vesicles in CHO cells. *J Cell Biol* **125**, 1015–1024.

Hobom, U., Brune, W., Messerle, M., Hahn, G. & Koszinowski, U. H. (2000). Fast screening procedures for random transposon libraries of cloned herpesvirus genomes: mutational analysis of human cytomegalovirus envelope glycoprotein genes. *J Virol* **74**, 7720–7729.

Hu, C., Hardee, D. & Minnear, F. (2007). Membrane fusion by VAMP3 and plasma membrane t-SNAREs. *Exp Cell Res* **313**, 3198–3209.

Jahn, R. & Scheller, R. H. (2006). SNAREs–engines for membrane fusion. *Nat Rev Mol Cell Biol* **7**, 631–643.

Jahn, R., Lang, T. & Südhof, T. C. (2003). Membrane fusion. *Cell* **112**, 519–533.

Kawabata, A., Jasirwan, C., Yamanishi, K. & Mori, Y. (2012). Human herpesvirus 6 glycoprotein M is essential for virus growth and requires glycoprotein N for its maturation. *Virology* **429**, 21–28.

Koshizuka, T., Ota, M., Yamanishi, K. & Mori, Y. (2010). Characterization of varicella-zoster virus-encoded ORF0 gene–comparison of parental and vaccine strains. *Virology* **405**, 280–288.